

<https://doi.org/10.1038/s41522-024-00643-0>

Irrigation of the intramedullary channel improves outcome of DAIR in a sheep model



Claudia Siverino¹, Lena Gens¹, Tim Buchholz¹, Caroline Constant¹, Manuela Ernst¹, Dominic Gehweiler¹, Mario Morgenstern², R. Geoff Richards¹, Henning Richter³, Niels Vanvelk¹, Maja Waschk³, Markus Windolf¹, Stephan Zeiter¹ & T. Fintan Moriarty^{1,2}✉

The management of fracture-related infection (FRI) with Debridement, Antibiotics, Irrigation, and Implant Retention (DAIR) is an appealing option, but its suitability is restricted to a relatively narrow proportion of patients. This study aimed to create a large animal model of DAIR after FRI and to evaluate outcomes after early (2 weeks) and delayed (5 weeks) DAIR. Additionally, intramedullary lavage (IML) of the intramedullary canal (IMC) is introduced as a novel technique to remove infected tissue. Our findings showed that DAIR failed to resolve infections in both early and delayed groups, whilst IML significantly reduced bacterial counts, leading to culture-negative results in the soft tissue and bone marrow. IML did not compromise long-term bone healing as revealed by an implant load sensor on the plate. In conclusion, DAIR was successfully achieved in a new large animal model with minimal losses. The IML method improves treatment efficacy, potentially broadening the range of patients suitable for DAIR.

Fracture-related infection (FRI) represents one of the major complications in orthopedic and trauma surgery¹, occurring in up to 30% of cases, depending on the severity of the injury². The most prevalent pathogen is *Staphylococcus aureus*, causing up to 40% of cases³. Recently an international consensus group established a standardized definition and recommendations for diagnosis and treatment of FRIs⁴. Despite recent progress, evidence for current management approaches is still scarce⁴. The principles behind FRI management are removal and excision of dead tissue and non-living material, providing stable bone fixation, dead-space management, sufficient soft tissue coverage and administering antimicrobial therapy. Based on these principles, the two main surgical treatment strategies for FRI are: debridement, antimicrobial therapy, and implant retention (DAIR) or implant removal/exchange⁵. Implant retention (DAIR) is the preferred approach whenever possible, as it is associated with less invasive procedures, fewer surgical interventions, and shorter hospital stays⁶. However, the incidence of treatment failure associated with DAIR is higher than that observed with implant removal⁷, particularly when patient selection criteria are not carefully considered. Deciding between these two surgical regimes depends on multiple factors such as the duration of infection, stability of the osteosynthetic construct, vitality of the bone and soft tissues, as well as the possibility of performing

debridement to reduce the bacterial load¹. Historically, FRIs were classified as early, delayed, or late infections with a cut-off at 3 and 10 weeks after fracture fixation^{8,9}. In “early” FRIs cases, fracture healing is generally still ongoing, hence the complete removal of the implant is often not an option. In this situation, DAIR is a tempting approach, allowing infection eradication and ensuring the stability of the osteosynthetic construct^{6,10}. In contrast, longer infection periods are associated with a more mature biofilm, increasing osteolysis and necrosis of the affected bone. Therefore, one of the more critical and evidence-based factors determining DAIR success is the duration of infection symptoms. A systematic review on the influence of duration of infection on the outcome of DAIR in FRI reported high success rates (86–100%) for DAIR revision surgeries within 3 weeks, while for late FRIs, the rate drops down to 67%⁹.

A major blockade to the further application of DAIR is that the intramedullary canal (IMC) cannot be debrided with implants in situ. Conventional intramedullary debridement involves invasive reaming of the IMC, which has been confirmed to improve infection management but requires removal of the implant to allow access to the reamer¹¹. Since implants are retained with the DAIR approach, and reaming is not an option, the fear of leaving highly infected tissue in situ is a primary factor discouraging surgeons from performing DAIR.

¹AO Research Institute Davos, Davos Platz, Switzerland. ²Center for Musculoskeletal Infection, Department of Orthopaedic and Trauma Surgery, University Hospital Basel, Basel, Switzerland. ³Clinic for Diagnostic Imaging, Department of Clinical Diagnostics and Services, Vetsuisse Faculty, University of Zurich Switzerland, Zurich, Switzerland. ✉e-mail: fintan.moriarty@aofoundation.org

In this study, we investigate intramedullary lavage (IML) of the IMC as a means to remove infected tissue from the IMC whilst retaining the implant. First, a large animal model of FRI with plating osteosynthesis, including a DAIR approach, was established, comparing early and delayed DAIR treatment outcomes in those time-dependent infections. It was observed that the conventional treatment failed to clear the infection in both the early and delayed DAIR groups and that the longer duration of the infection caused the bacteria to reside within the deeper niches of the bone and implant. The use of the IML approach resulted in a significant reduction in bacterial burden compared to the standard DAIR approach, with bone marrow and soft tissues being completely culture-negative. The load sensor integrated into the implant plate successfully tracked delayed healing resulting from infection and confirmed that IML does not adversely affect long-term bone healing.

Results

Animal welfare and clinical observations

In total, 17 sheep were included in this study (Fig. 1). All included animals recovered well from surgery and anesthesia; however, they all required intensive post-operative care, particularly in the first days after revision surgery. Most animals needed frequent additional pain management, particularly in the sheep receiving the intramedullary inoculation (3 weeks groups). Details on animal welfare and clinical observation are described in Supplementary Material (Results) Supplementary Table. 1 and Supplementary Fig. 1. Six animals were operated on but excluded from the study, due to infection-induced wound dehiscence, a predefined exclusion criterion or because at revision surgery the fascia could not be sutured. The excluded animals belonged to the 5 weeks ($n = 2$) and 3 weeks groups ($n = 2$, 3 weeks and $n = 2$, 3 weeks + IML), indicating no single group was more adversely affected.

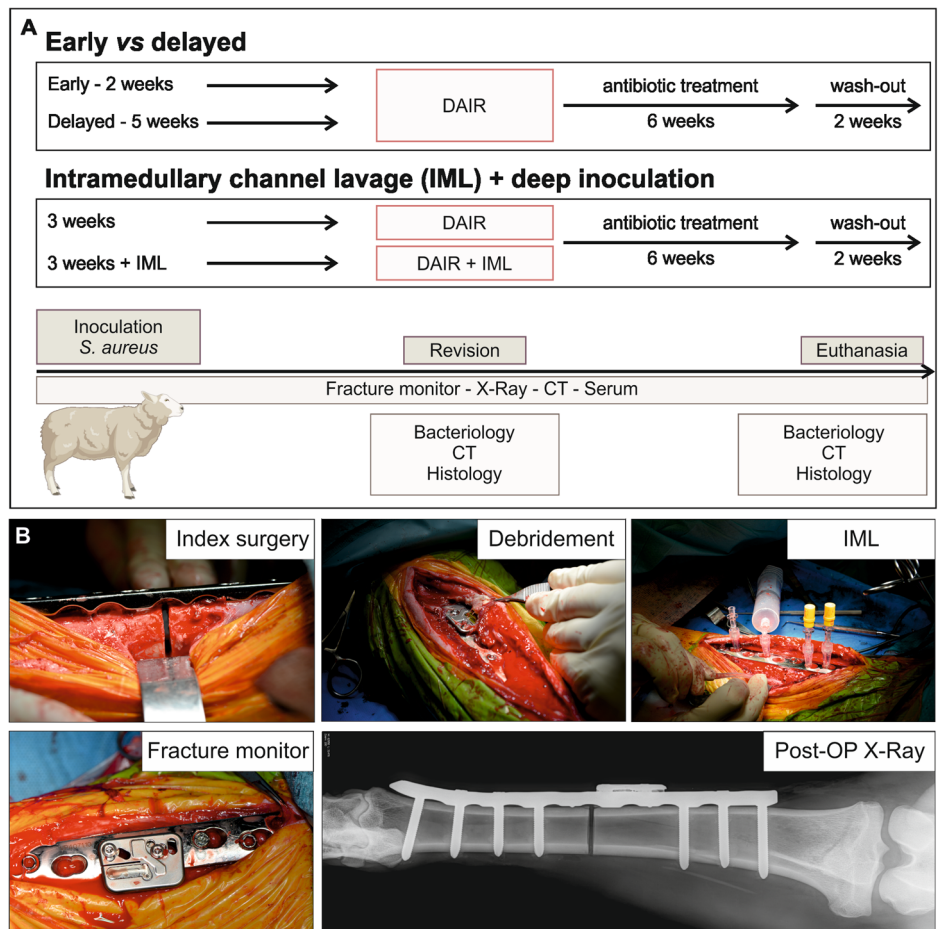
Early versus delayed infection

Quantitative bacteriology. In the early *versus* delayed comparison, 2 or 5 weeks after initial inoculation, the same DAIR approach was performed for both groups, and quantitative bacteriology was performed on debridement tissue (Deb T.) and irrigation fluid (Irr. Fluid). At revision surgery, colony forming unit (CFU) values were broadly equivalent in each sampled location (Deb. T and Irr. Fluid, independent of the infection period, $p = 0.62$ Deb T. and $p = >0.99$ Irr. Fluid) (Fig. 2A).

At euthanasia, animals from the early, 2 weeks infection group were all (3/3) culture positive (Fig. 2B), although there was substantial intra-group variability in CFU values. In the delayed, 5 weeks infection group, three of the four animals were culture positive in all the collected samples (Fig. 2B). CFU values were comparatively similar within this group, and higher numbers of bacteria were recovered from deeper tissues such as bone marrow, compared with the overlying subcutaneous tissue (S. Tissue).

Histopathology. At euthanasia, bone samples were collected from the osteotomy/callus area to compare healing and signs of infection in both groups. The osteotomy in the sheep of the early group was still clearly visible (Fig. 2C) and was filled with highly vascularized fibrous tissue, and newly formed trabecular bone was limited to the blunt end of the osteotomy (non-bridging defect). In the delayed group, where DAIR was performed after 5 weeks, bone formation across the osteotomy appeared more advanced, with less fibrous tissue, and areas with high osteoblastic activity and a higher rate of remodeling (shown by the darker pink areas) (Fig. 2D ii) and the presence of hyaline cartilage (Fig. 2D i). The more advanced bone formation is in keeping with the difference in the total duration of the study (11 weeks *vs* 13 weeks for early and delayed groups

Fig. 1 | Study outline and surgical details. **A** Study outline—group outline, treatments, and outcome measures of the study. Outcome measures at the specific time points: bacteriology, clinical computed tomography (CT), and histopathology at revision and at euthanasia including contact radiograph. Continuous monitoring of fracture healing using the fracture monitor and weekly X-Rays and serum. **B** Surgical details: creation of the 2 mm osteotomy during initial surgery; surgical site at DAIR revision surgery in the early cohort; IML approach performed at revision; fracture monitor application on the plate; representative X-ray of tibia post-OP.



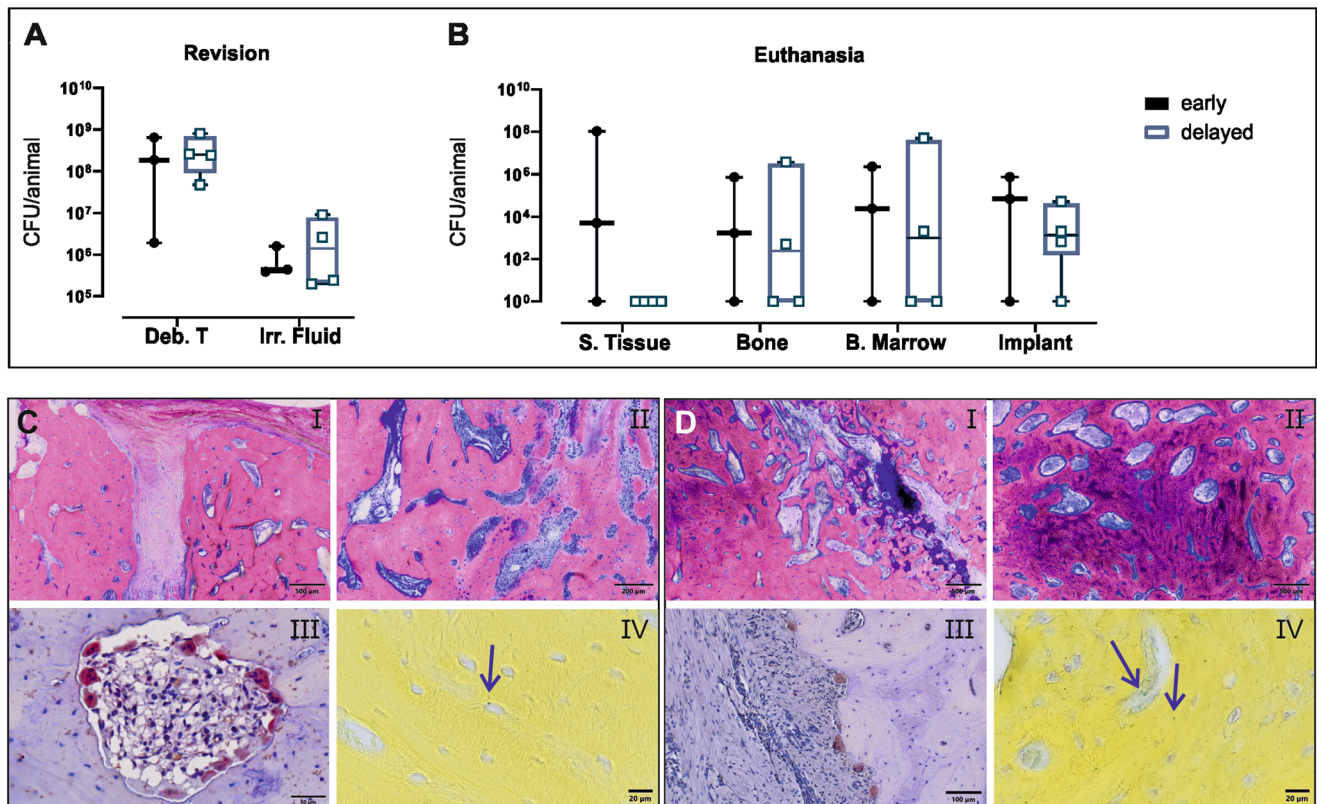


Fig. 2 | Bacteriological and histopathological evaluation of early versus delayed DAIR. **A** Sheep was infected with *S. aureus* MSSA for either 2 (early, $n = 3$) or 5 weeks (delayed, $n = 4$). **A** Quantitative bacteriology of samples collected during DAIR revision surgery after 2 weeks or 5 weeks of infection. **B** Quantitative bacteriology of samples collected at euthanasia, 8 weeks after revision surgery. Culture-negative samples were arbitrarily assigned a value of 1 for the purposes of displaying on a \log_{10}

axis. Individual data points are shown including median value and range. Statistical analyses were performed using the Mann–Whitney test. **C, D** Representative histology images of the **C** early and **D** delayed groups. After euthanasia, the tibia was dissected, and the bone cores from the osteotomy area were processed for histology and stained by G&E (i, ii), TRAP (iii), and BB (iv) staining. Arrows in BB-stained sections indicate *S. aureus*. Scale bars, (i) 500 μm , (ii) 200 μm , (C iii) 50 μm , and (D iii) 100 μm , (iv) 20 μm .

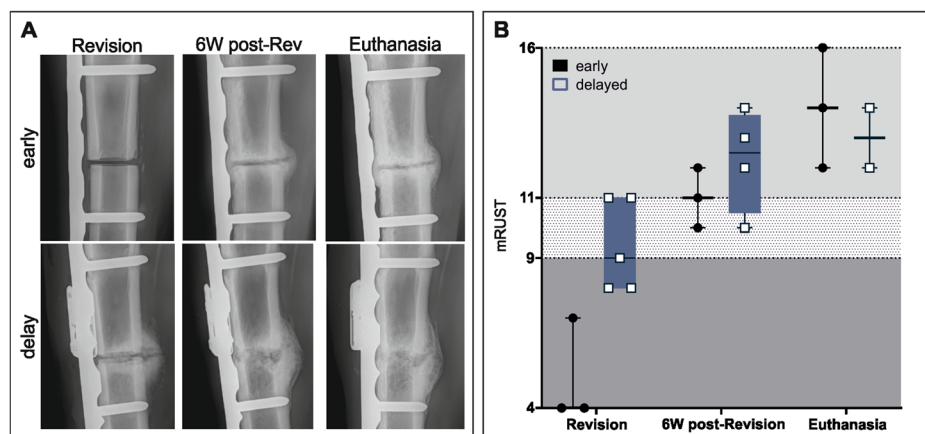


Fig. 3 | Radiographic evaluation of early vs delayed DAIR groups using the mRUST at revision, 6 weeks from revision, and at euthanasia. **A** Radiographs of representative animals from the 2 weeks ($n = 3$) and 5 weeks infection period ($n = 4$). Radiographs show a defect area between the proximal and distal screw pre-revision surgery, at 6 weeks post-revision, and at euthanasia. Time points differ between the two groups according to the infection period. For the early group, revision (2 weeks), 6W post-Rev (8 weeks), and euthanasia (10 weeks), while for the

delayed group, revision (5 weeks), 6W post-Rev (11 weeks), and euthanasia (13 weeks). **B** The mRUST score indicates 3 areas: non-union <9, possible non-union >9 and <11 and healing >11⁷. In the delayed groups $n = 2$ animals had to be euthanized 1 week before the other 2 animals were included in the mRUST graph, therefore not included for the euthanasia mRUST evaluation. Individual data represented including median value and range. Statistical analyses were performed using Mann–Whitney test.

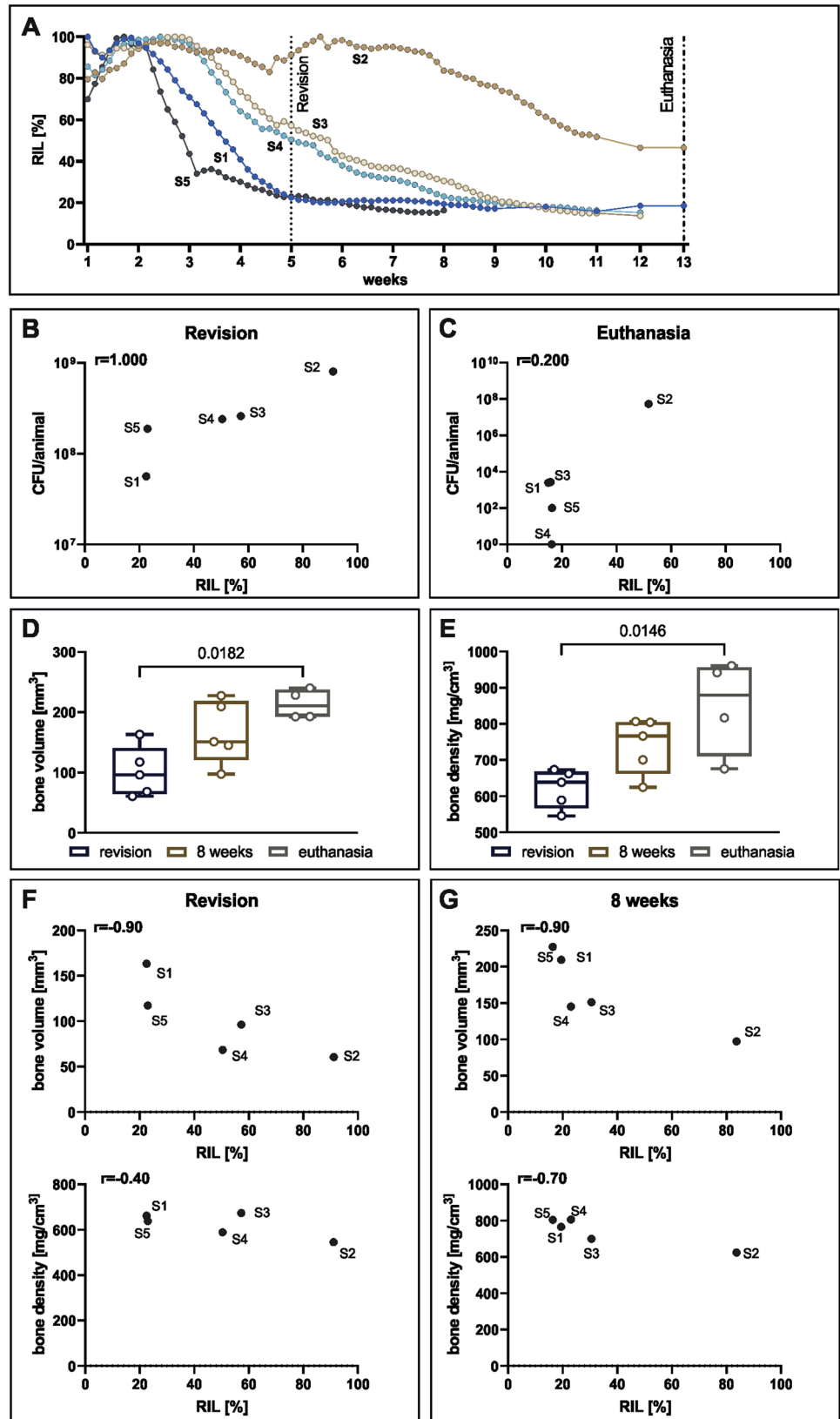
respectively). Scattered osteoclasts and bacteria within the osteocyte lacunae were observed in both groups (Fig. 2C, D iii, iv).

Radiographic evaluation of healing in early and delayed DAIR. Regular radiographs were taken from sheep in both the early and delayed

groups over the entire duration of the study (Fig. 3). Substantial differences were observed at the time of revision (2 or 5 weeks). Animals from the early group show a small callus over the still visible osteotomy with minimal signs of osteolysis in the proximal and distal screws close to the osteotomy area (Fig. 3A). The animals from the 5 weeks infection group

Fig. 4 | Relative implant load (RIL) data measured by the fracture monitor in the delayed group.

A RIL over 13 weeks of the infected animals from the delayed group ($n = 5$). B correlation of RIL and CFU at revision ($n = 5$). C Correlation of RIL and CFU at euthanasia. D Evaluation of bone volume and E bone density within the 2 mm of osteotomy. Individual data represented including median value and range. Statistical analyses were performed using Dunn's multiple comparisons test. F Correlation of bone volume and bone density data obtained from the clinical CT with sensor data at 5 weeks and at G. 8 weeks. Spearman correlation values (r) are indicated in the correlation graphs.



show an increased callus area over the osteotomy but with more osteolysis visible around the screws close to the osteotomy (Fig. 3A). The mRUST score revealed differences between the early and delayed groups at revision, showing higher scores for the delayed groups compared to the early group, mainly due to the difference, 2 *versus* 5 weeks, from index surgery.

However, at 6 weeks post-revision, both groups had reached a similar state of healing. After a further 2 weeks of wash-out, bone healing had not progressed further for either group (Fig. 3B).

Healing progression was also monitored using the implant load sensor (fracture monitor) in 5 animals from the delayed group only (Fig. 4A).

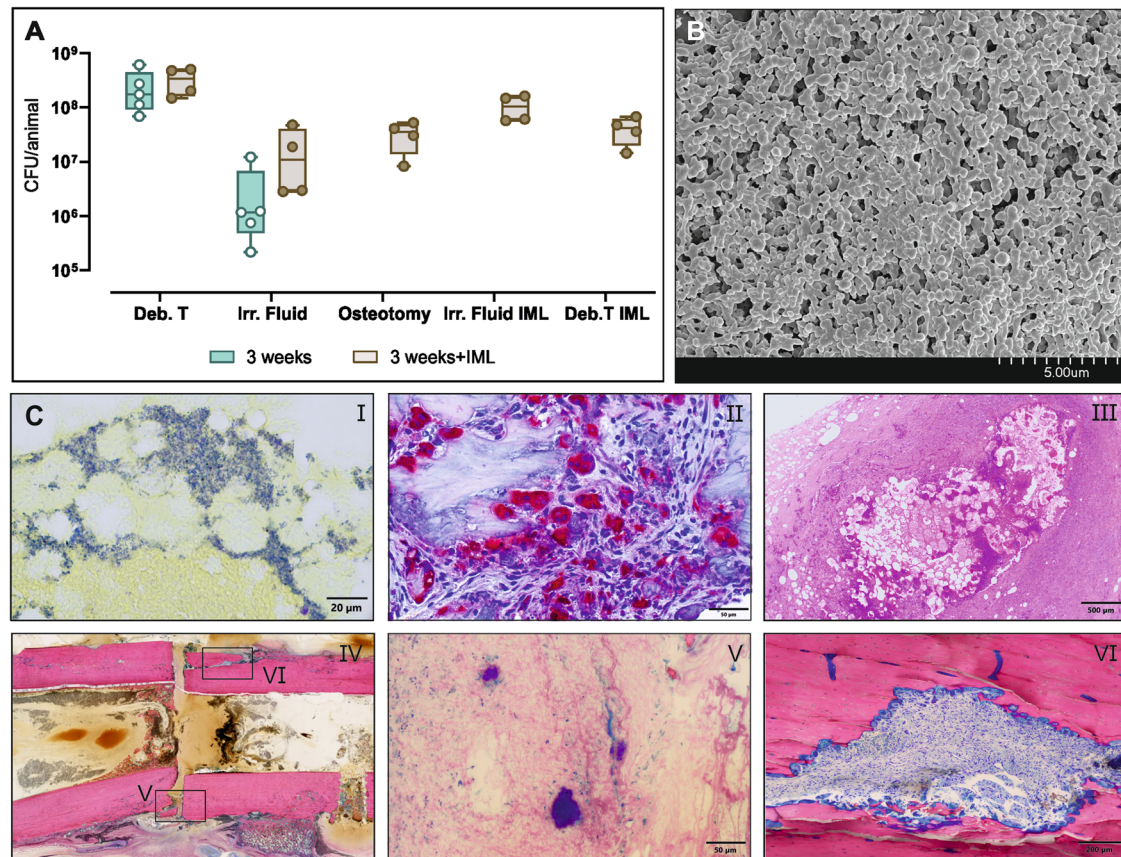


Fig. 5 | Bacteriology and histopathology at revision after 3 weeks infection period. Sheep were infected with *S. aureus* MSSA for 3 weeks using the collagen sponges ($n = 9$ in total), and at revision $n = 5$ received the normal DAIR approach while $n = 4$ received DAIR + IML. **A** Samples were collected during DAIR revision surgery with and without the IML. In the 3 weeks group: Osteotomy, Irr. Fluid IML and Deb. T IML are not collected since standard DAIR is performed. Individual data represented including median value and range. Statistical analyses were performed using Mann–Whitney test. **B** SEM of the plate at revision after 3 weeks of infection.

C (i) BB staining, (ii) TRAP staining and (iii) H&E staining of the bone marrow collected from excluded animals euthanized the day after revision surgery. (iv) Overview of the defect area at revision after 3 weeks using G&E staining with details on gap, (v) bacterial microcolonies and (vi) osteoclast in the sequestrum. The samples used for histology were obtained from sheep excluded from the study after 3 weeks of infection. Scale bars (i) 20 μm, (ii) 50 μm, (iii) 500 μm, (iv) 5 mm, (v) 50 μm, (vi) 200 μm.

Relative implant load (RIL) values show three different healing patterns over time (Fig. 4A): a more rapid healing with RIL below 40% after 4 weeks (S1 and S5 in Fig. 4A); a delayed healing with RIL around 60% at 4 weeks (S3 and S4 in Fig. 4A); and a non-healing scenario with RIL still at 60% by the end of the study (S2 in Fig. 4A). These data were correlated with the CFU values at revision and at euthanasia (Fig. 4B, C), with high correlation at revision ($r = 1.000$), measured between bacterial count and implant load. Bone volume and bone density were measured at the same time points by CT, with increasing values over time in both groups (Fig. 4D, E). Bone volume and density linearly correlate with RIL at revision and at 8 weeks (Fig. 4F, G). Only two animals reached the 13 weeks, therefore no correlation graph is shown for bone volume and density/RIL at euthanasia.

Deep bone infection with or without IML

Bacteriology at revision. During the inoculation surgery of animals in these groups, collagen sponges with *S. aureus* were used to induce a deeper, more consistent bone infection. These animals received treatment with or without an additional IML concept, designed to debride the IMC that is not normally debrided in a DAIR approach. Videos of the IML approach are available in the Supplementary material (Supplementary Video 1 and 2).

The debrided material collected during the conventional DAIR approach (without IML) after 3 weeks showed high bacterial count in the range of 10^8 CFU/animal and 10^6 CFU/animal in the debridement tissue and in the irrigation fluid, respectively (Fig. 5A). These values are within the

same range of the 2- and 5 weeks infection groups shown above. The DAIR with IML provided additional debridement material from inside the IMC. These samples yielded a high bacterial burden with values above 10^7 CFU/animal in all the samples (Fig. 5A). The screws collected during the IML approach had approximately 7×10^5 CFU/screw.

Histopathology of deep infection after 3 weeks. The revised inoculation protocol for the deep bone infection resulted in substantial infection, as revealed not only quantitatively by bacterial culture but also by histopathology. Scanning electron micrographs of the plate after 3 weeks, showed a dense biofilm formation over the plate (Fig. 5B). The presence of substantial numbers of bacteria within the bone marrow was confirmed by BB staining of material removed from the IMC (Fig. 5C i). The material in the IMC was found to display abundant TRAP-stained osteoclasts in the bone marrow (Fig. 5C ii). The presence of a chronic encapsulated abscess with fibroblastic capsule, degenerating neutrophilic granulocytes, fatty cells necrosis with cholesterol crystals, and bacterial colonies was detected by H&E staining (Fig. 5C iii). The overview of the defect area shows that the defect is still clearly defined with sequestrum created during surgery (identifiable by the sharp edges) (Fig. 5C iv). Additionally, bacterial microcolonies were observed within the defect close to the bone sequestrum (Fig. 5C v) and large amounts of osteoclasts were visible in an intra-cortical fracture line near the osteotomy in the upper part of the defect (Fig. 5C vi).

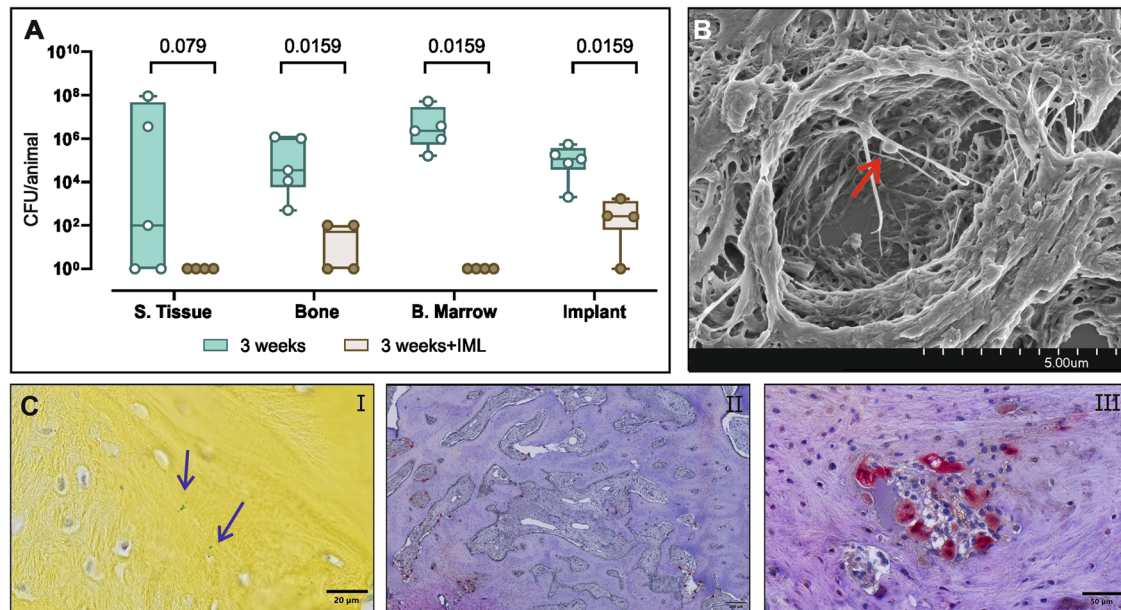


Fig. 6 | Bacteriology and histology of bacteria at euthanasia in sheep with 3 weeks infection. **A** Sheep were infected with *S. aureus* MSSA for 3 weeks using the collagen sponges ($n = 9$ in total). At revision surgery sheep received either the classical DAIR approach ($n = 5$) or the DAIR with the IML ($n = 4$). After 6 weeks of systemic antibiotics and 2 weeks of additional wash-out, the animals were euthanized, and samples from the infected tibia were processed for bacteriology and histopathology.

Culture-negative samples were arbitrarily assigned a value of 1 for the purposes of displaying on a log₁₀ axis. Individual data represented including median value and range. Statistical analyses were performed using Mann Whitney test. **B** SEM image of bacteria (indicated by the red arrow) within the osteocyte lacuna, **C** BB-stained (i) and TRAP-stained (ii, iii) sections of the bone defect area. Scale bars (i) 20 μ m, (ii) 200 μ m, (iii) 50 μ m.

In vitro cytotoxicity and antibacterial activity of TPA. During the IML approach, tPA was used for its proteolytic action against the dense structure formed inside the IML during the 3 weeks of infection. The effect of tPA was also tested in vitro to better evaluate its effects on cells and bacteria. Human fibroblasts were exposed to different concentrations of tPA (Supplementary Fig. 2). The concentration of tPA used in vivo, 1 mg/ml and lower (0.1 and 0.01 mg/ml) did not show any effects of fibroblasts viability at any time point. The highest concentration used, 10 mg/ml, resulted in decreased cellular metabolic activity after 24 h ($p = 0.0362$ and 0.0119 , compared to 0.1 and 0.01 mg/ml, respectively). In vivo, tPA was injected and let to act for 10 min and afterwards flushed with saline. Additionally, tPA showed no effects on biofilm grown on metal discs and exposed to flucloxacillin (same used in vivo systemically for the first two weeks) (Supplementary Fig. 2). In this biofilm assay only the antibiotic tobramycin, included as a control, showed significant reduction in bacterial count.

Thoracic CT and blood culture after IML. Lung angiograms were performed on sheep during DAIR with and without IML in order to determine whether fat emboli reached the lungs directly after revision surgery, 7/8 sheep (both 3 weeks groups with and without IML) showed filling defects in the pulmonary arteries (Supplementary Table 2). The larger primary arteries were affected in 4/5 sheep in the control group and 0/3 in the lavage group. Secondary arteries were affected in 4/5 of the sheep in the control group and 1/3 of the sheep in the lavage group. Tertiary arteries were affected in 5/5 sheep in the control group and 2/3 in the lavage group. Three days later, filling defects in the large primary pulmonary arteries had dissolved in 3/4 sheep, while they developed in one sheep in the lavage group. In the secondary pulmonary arteries, the filling defects dissolved in 4/4 sheep in the control group and 1/1 sheep in the lavage group. In comparison, they were present in the one sheep of the lavage group that was not analyzed immediately post op. In the tertiary arteries, the filling defects dissolved in 1/5 of the sheep in the control group and 1/2 of the sheep in the lavage group. In the analysis of further lung changes, all sheep showed signs of atelectasis or other underlying

lung pathologies preoperatively, making it difficult to assign further changes to the filling defects or other pathologies related to the lavage.

To assess the possibility that the IML approach could cause dispersion of bacteria in the blood circulation, blood cultures were performed at prior to revision surgery, before IML, post-IML, and 4 h post-IML. Cultures were examined at 24 h and after 1 week. No *S. aureus* was detected in the bloodstream at any time point.

Quantitative bacteriology. Consistent with the findings from both the early and delayed groups previously described, conventional DAIR approach performed after 3 weeks of deep infection failed to eradicate the infection in all the tissues (Fig. 6A), with high bacterial burden with CFU counts between 10^4 and 10^6 in most samples. The animals receiving the IML approach showed complete eradication of the infection in the S. Tissue and B. marrow ($p = 0.079$ and $p = 0.0159$). The detected bacteria in the culture-positive samples (2/4 of the bone samples and 3/4 of the implant) are significantly lower ($p = 0.0159$ and $p = 0.0159$) compared to the classic DAIR approach (Fig. 6A). At euthanasia, 5/5 animals from the control group (classic DAIR) and 3/4 from the IML group were culture positive. Representative images of the 3 weeks group without IML show the presence of bacteria within the osteocyte's lacunae (SEM and BB staining, Fig. 6B, C i) and a high osteoclastic activity (Fig. 6C ii, iii) within the bone sample isolated from the osteotomy area. No bacteria were found in the BB-stained sections of the IML group.

Histopathology. Bone healing in the 3 weeks deep infection animals with conventional DAIR and DAIR with IML was evaluated radiographically and compared using mRUST at revision, 6 weeks after revision, and at euthanasia (Fig. 7A, B). Increased radiolucency can be noticed around the screws in the 3 weeks infection group compared to the 3 weeks+IML at euthanasia (Fig. 7A, B, euthanasia). At revision, all animals had similar mRUST scores since they had identical conditions up to that time. During DAIR + IML, the osteotomy was refreshed to allow a proper debridement of the IML. At 6 weeks post-revision, animals receiving IML had lower scores compared to those receiving the standard DAIR approach

Fig. 7 | Radiographic evaluation of the 3 weeks infection groups with and without IML at revision, 6 weeks from revision, and at euthanasia using the mRUST. A, B Radiographs of representative animal from the 3 weeks ($n = 5$) and 3 weeks+IML ($n = 4$). Radiographs show a defect area between the proximal and distal screw pre-revision surgery, at 6 weeks post-revision, and at euthanasia. For the animals of the 3 weeks + IML the osteotomy was refreshed during revision surgery. **C** The mRUST score indicates 3 areas: non-union <9, possible non-union >9 and <11 and healing >11. Individual data represented including median value and range. Statistical analyses were performed using Mann–Whitney test. **D, E** Histology images show G&E-stained sections of the bone defect area of the 3 weeks (**D**) and 3 weeks+IML (**E**) group. Scale bar in **D, E** 2 mm.

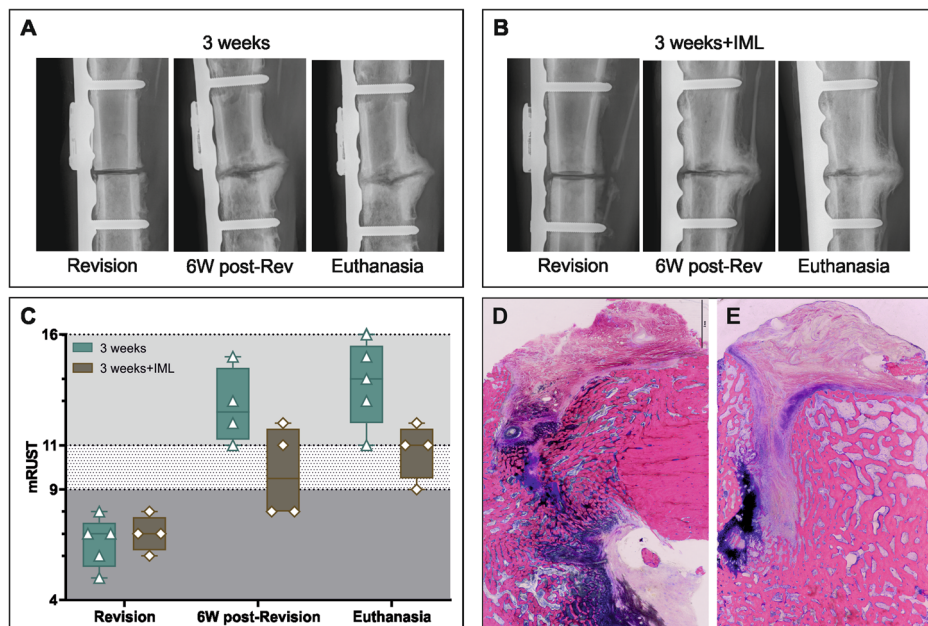


(Fig. 7C). The same trend was observed at euthanasia, where mRUST values of IML group were again lower (Fig. 7C).

Based on histopathology, the 3 weeks group presents an increased bone remodeling with highly vascularized tissue and highly active osteoblasts (Fig. 7D). While in the 3 weeks+IML groups, more newly formed trabecular bone is visible (Fig. 7E). However, in both cases histopathology shows a still visible defect line filled also with remnants of dark azure-blue stained hyaline cartilage (Fig. 7D, E). In case of the 3 weeks group with IML, few signs of ongoing osteochondral bone formation are observed close to the hyaline cartilage (Fig. 7D).

Bone healing in the animals from both 3 weeks infection period groups was also monitored using the fracture monitor (Fig. 8). In case of the standard DAIR approach, the relative implant load values start to decrease within the first 3 weeks post-op and reaching a RIL around 20% at the end of the study. Only one animal shows an increase in RIL after the revision surgery, but at euthanasia the RIL is similar to those of the other animals (Fig. 8A). The two animals from the 3 weeks + IML group show higher RIL after revision due to the refreshment of the osteotomy but ultimately reach also similar RIL at the end of the study ~20% (Fig. 8A). RIL and bacteriology results do not show any correlation at revision (Fig. 8B), while at euthanasia the RIL and the bacterial count correlate ($r = 0.68$), with the two animals receiving the IML and having the fracture monitor showing the lowest RIL and bacterial count (Fig. 8C). Evaluation of bone volume and bone density overtime shows a big variation in bone volume and density in both groups at 8 weeks and at euthanasia (Fig. 8D, E).

Discussion

Managing FRI with implant retention (DAIR) is an appealing approach for both patients and surgeons alike due to time and cost savings, and reduced burden for the patient. At the present time, however, the patient populations for whom DAIR is indicated are rather narrow due to poor outcomes for patients not fitting the current criteria. Broadening the range of patients suitable for DAIR would be a major improvement in patient care. Unfortunately, novel approaches to broaden eligibility criteria for DAIR have not been introduced in recent years despite the obvious potential benefits.

In order to address this unmet clinical need, we devised an IML protocol involving flushing the IMC with saline to remove the deeper antibiotic-recalcitrant nidus of infection. The bacterial burden removed using this approach was substantial, and histology revealed that this IMC otherwise contains large collections of bacteria, including microcolonies embedded in

abscesses with fibroblastic capsule within the IMC. Removal of these bacteria was responsible for negative cultures in the soft tissue and in the bone marrow. This dramatic improvement in the bone marrow was achieved without the need for any mechanical reaming, implant removal, or prolongation of antibiotic therapy.

The implementation of IML resulted in a significant decrease in bacterial load, particularly in the IMC and soft tissue, but also a reduction of 3 to 4 log₁₀-fold changes from the bone and implant compared to the control group. The benefit of IML can also be noticed by the differences in radiolucency around the screws in the group with IML compared to control, which we attribute to superior infection management. The importance of these few remnant bacteria on the implant or in the bone cannot be conclusively determined, but they are possibly antibiotic-tolerant and primed to cause reinfection. Therefore, additional therapy, such as local antibiotics, may be required for infection eradication.

One critical step of the IML approach was to refresh the osteotomy during lavage. This was done to facilitate the flushing but is generally contraindicated in surgical practice. Standard clinical dogma is that if healing is progressing, it should be supported even in the presence of an infection. This is due to the fact that after completion of healing, implant removal may be performed, and infection eradication is easier in the absence of the implant (biofilm). At 6 weeks after revision, fracture healing is delayed compared to controls that did not receive the refreshment of the osteotomy. However, considering the fracture monitor data, the relative implant load at the end of the study indicates similar values between the IML group and those with the conventional DAIR. Similarly, histology and radiography do not indicate healing is compromised, but rather restarted due to the refreshing of the osteotomy. A longer observation period of the animals with the refreshed osteotomy is, therefore, expected to result in complete healing of the fracture, with the critical benefit of better infection management. Amongst the most obvious potential complications of IML are the creation of fat emboli or the seeding of bacteria into the bloodstream^{12,13}. Neither emboli nor bacteremia was observed in this study, suggesting the IML is a safe approach. However, dedicated safety studies would be required in the future to provide more in-depth analysis.

Aside from the obvious impact of IML, this study also investigated the importance of duration of infection on DAIR outcome. The data from human patients shows trends for poorer outcome after ~10 weeks duration^{9,14}. Our study indicated no substantial differences in treatment outcome for DAIR at 3 or 5 weeks. Nevertheless, the results clearly showed

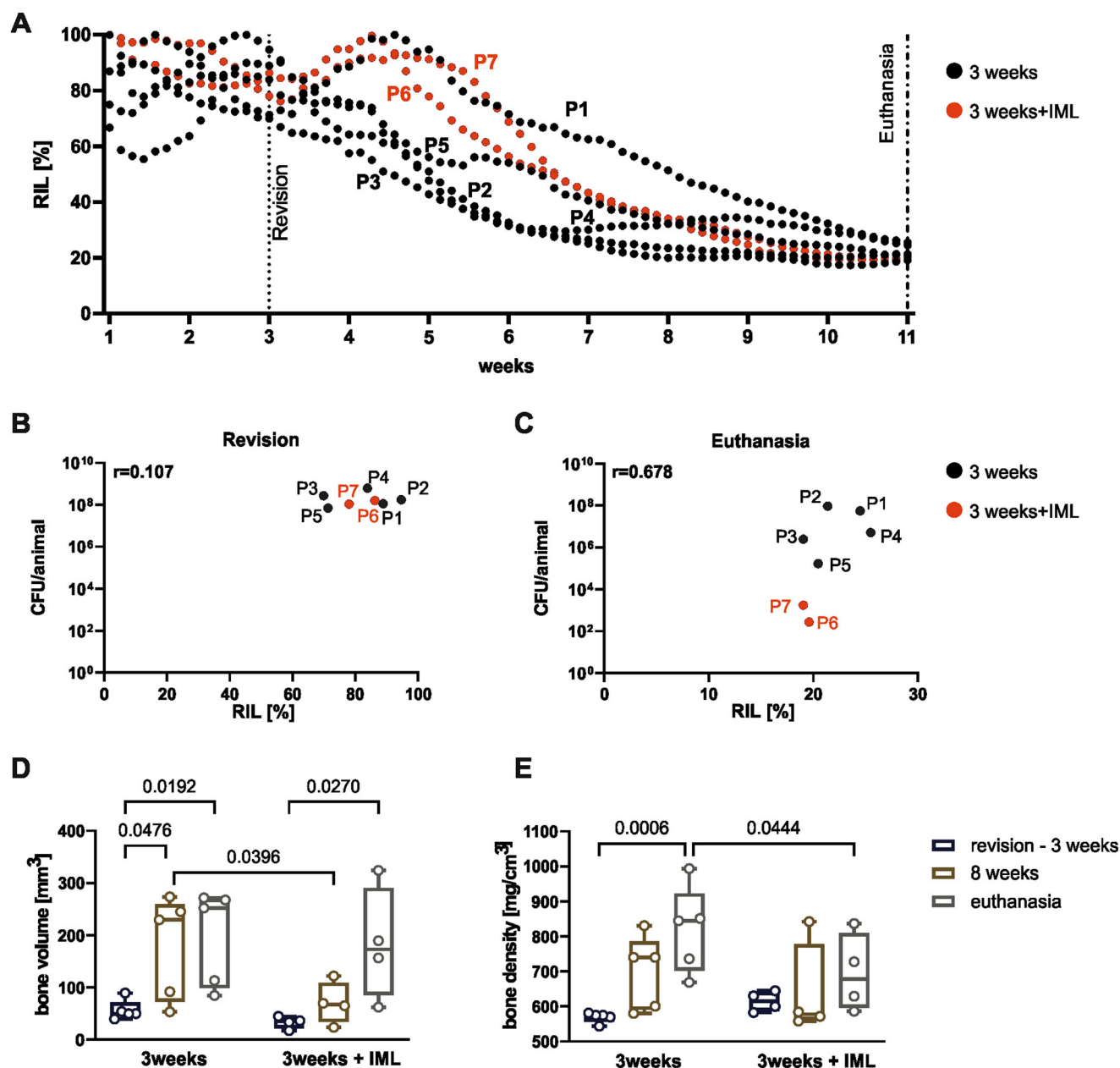


Fig. 8 | Relative implant load (RIL) data measured by the fracture monitor. A RIL over 11 weeks of the 3 weeks infected ($n = 5$, black) and 3 weeks + IML ($n = 2$, red) animals. **B, C** Correlation of RIL and CFU at revision and at euthanasia, respectively. **D, E** Evaluation of bone volume and bone density within the 2 mm of osteotomy in

the 3 weeks and 3 weeks + IML groups. Individual data represented including median value and range. Statistical analyses using 2-way ANOVA with Šidák's multiple comparisons test. Spearman correlation values (r) are indicated in the correlation graphs.

the retraction of the infection away from softer, more superficial tissues and persistence in deeper niches such as the bone and implant as the infection duration increased. The persistence of bacteria within the osteocyte canalicular network has already been shown in previous studies, representing another mechanism of bacterial evasion in FRI^{15–17}. This is consistent with findings in a rabbit model¹⁸, which also showed retraction of the infection in a delayed DAIR settings (4 weeks infection) compared to the early DAIR approach at 1 week. Based on the consistency of this finding across studies, it seems that the bacteria are more readily eradicated in soft tissues where vascularity may be superior, antibiotic penetration consequently also improved, and there is also ready access to immune cells. The infection then can only persist in the biofilm on the plate, or within dense, fibrotic abscess-like structures deep within the IMC. These are the deep nidus of infection that could not be eradicated by conventional DAIR. In order to successfully flush the IMC, we required an initial application of the thrombolytic and

fibrinolytic serine protease tPA to loosen up the fibrotic tissue in the IMC and allow later flushing. Under in vitro conditions, the tPA did not independently have an antibacterial effect or cytotoxic effect, but its fibrinolytic functionality allowed the IMC to be easily flushed out and collected. Dedicated instrumentation to facilitate flushing of the IMC without the addition of the tPA, or even without requiring refreshing the osteotomy, would represent two aspects of this IML approach that could be most constructive for later clinical implementation.

This study also revealed the potential of measuring implant load as a surrogate for fracture healing. The use of sensors for measuring implant load as an objective and quantitative indicator of fracture stability can provide valuable information on the progression of healing¹⁹. Clinically, such sensors have been used with internal²⁰ and external fixators²¹ in difficult lower limb fractures and proved to be capable of tracking the course of healing and differentiating between healing status. In contrast to passive approaches,

such as the strain-gauge sensors which require a reference measure and rely on manual execution of the measurements, an active and continuous monitoring was proposed by Windolf et al. in the last years^{21,22}. In this study, the fracture monitor could track the implant load as the infection was induced and treated and monitor the impact of the IML. Implant load over seemed to correspond to the degree of infection burden, with high correlation values between the bacterial load at revision and at euthanasia and the sensor data. The implant load could identify the infected animals, measuring the highest RIL values in the culture-positive animals at the end of the study and identifying delayed healing associated with infection. Such data were never shown before and prove that constant monitoring of fracture healing using a sensor could help the earlier diagnosis of delayed fracture consolidation due to infection.

In conclusion, this large animal model of FRI, including DAIR revealed the importance of deep bacterial reservoirs that contribute to infection persistence. Removal of the infected content of the IMC significantly contributed to the achievement of culture negativity in the bone marrow. IML is thus supportive of improved infection management whilst allowing implant retention and restarts bone healing without long-term impact on fracture healing.

Methods

Animals and study design

The study was approved by the Cantonal authorities in Graubünden, Switzerland, Permission # 07_2020, 22_2021.

Healthy, skeletally mature, female Swiss Alpine sheep ($n = 23$), 2–4 years of age, mean weight 73 kg (range 60–81 kg), were enrolled in this study. Sheep were chosen for this study because they allow the use of human-size fixation implants, surgical instruments and an antibiotic dosing regimen equivalent to human standard of care. Prior to inclusion in the study, the sheep were confirmed healthy based on a complete physical assessment performed by a veterinarian, a complete blood cell count, and were free of signs of orthopedic disorders and other diseases. Prior to the start of the study, the sheep were acclimatized to the animal holding facility for at least two weeks prior to the surgical procedure. The sheep were kept in groups under a 12 h dark/light cycle and fed with hay and mineral supplements with free access to drinking water. Only female sheep were included due to the limited availability of rams of this age.

Study design, including groups, and timeline for infection duration, revision surgery, and treatment, as well as outcome measures are shown in Fig. 1 and Supplementary Table 1. Sheep were allocated to their group only after completion of debridement at revision surgery and surgeons were blinded to the treatment group until revision surgery. Due to the staggered study design, no randomization was performed. The use of the staggered approach is based on the fact that the initial experimental findings dictated the following animal experiments, which could not be predefined due to the novelty of the model and the complexity of the research question. This stepwise approach was also based on welfare grounds, to ensure as few animals as possible were exposed to this high burden at the start of the study when the model was not yet established. The shortest infection time of 2 weeks was used to assess the course of infection and animal well-being, before proceeding to the longer infection and observation period. In order to minimize potential bias due to the staggered approach, dissection and bacteriology were performed for all the animals following the same protocol.

Surgery, revision surgery, and post-operative care

Surgery. The sheep were sedated with 0.04 mg/kg detomidine (Equisedan, Graeb, Switzerland) injected intramuscularly 30 min (min) before being transported to the surgical preparation room. Induction was done by intravenous (iv) injection of 0.2 mg/kg midazolam (Midazolam Sintetica, Sintetica, Switzerland) and 4 mg/kg ketamine (Ketasol 100, Graeb, Switzerland). Anesthesia was maintained using approximately 3% sevoflurane (Sevofluran Baxter, Baxter, Germany) in oxygen and air. Preemptive analgesia was conducted using lumbosacral epidural analgesia with 1 ml buprenorphine (Bupaq, Streuli Pharma AG,

Switzerland) mixed with 5 ml lidocaine (Lidocain 2%, Streuli Pharma AG, Switzerland), as well as non-steroidal anti-inflammatory drug with 1.4 mg/kg carprofen (Carprodolor, Virbac, Switzerland) injected iv. Each animal received 2.2 mg/kg ceftiofur (Excenel, Zoetis, Zürich, Switzerland) iv as a peri-operative antibiotic at least 30 min before the surgical incision of the first surgery. Antibiotics were only given after all bacteriological samples had been collected during the revision surgery.

The sheep were placed in the right lateral recumbency, and the right hind leg was aseptically prepared. A skin incision on the medial aspect of the right tibia was done followed by blunt subcutaneous preparation to expose the medial aspect of the tibial bone. The plate (10-hole 5.5 mm steel plate, DePuySynthes Inc.) was placed on the medial aspect of the tibia, its distal end approximately 2 cm proximal to the medial malleolus. For each surgery, the plate was manually pre-bent (distally between screw holes #8/9 and #9/10 to $\sim 10^\circ$) for better anatomical fit. Plate holes were drilled with a 4.3 mm drill bit, and the plate was fixed with 5.0 mm locking screws. A standardized transverse osteotomy was created by cutting the bone with an oscillating saw and custom-made jig, resulting in a gap width of 2 mm.

Placement of the fracture monitor. Animals from the delayed group with DAIR revision at 5 weeks and animals from the 3 weeks deep infection group with or without IML received the fracture monitor. Details are described below. This device was attached to the plate at screw holes #4 and #5, which were not occupied by locking screws.

Soft tissue infection. A total of 2.5 mL of saline solution containing 3×10^6 CFU of *Staphylococcus aureus* MSSA (ATCC 25923) was pipetted over the plate prior to closure. Two different observation periods prior to revision surgery were compared: 2 and 5 weeks ($n = 3$ and $n = 4$, respectively) to replicate early and delayed infection treatment.

Deep bone infection. The inoculation protocol was modified, and two collagen sponges (1/8 of TissuFleece E 3.6×1.8 cm, Baxter), each with 1×10^6 CFU *S. aureus* MSSA (ATCC 25923) were inserted through the osteotomy, one towards the proximal and one towards the distal part of the IMC. Additionally, 1 ml of 1×10^6 CFU *S. aureus* MSSA (ATCC 25923) was pipetted over the plate prior to closure (250 μ l on screw #3, 250 μ l on screw #7, 250 μ l on top of sensor, 250 μ l between plate and sensor (in animals without the sensor, 2×250 μ l on top of the plate in the same region)). The total inoculum was calculated as $\sim 2.5 \times 10^6 \pm 1.8 \times 10^6$ CFU/animal.

Fracture monitor. Animals from the 5 weeks infection group ($n = 5$), from the 3 weeks ($n = 5$) and 3 weeks + IML ($n = 2$) groups were equipped with a fracture monitor implant during the initial surgery (not available for the earlier group of 2 weeks infection and in the 3 weeks + IML group $n = 3$ fracture monitor did not properly function and had to be removed during revision surgery). The fracture monitor is an implant developed at the AO Research Institute Davos for continuous measurement of implant load as an indirect measure of fracture stability²¹. The implantable datalogger can be attached to conventional bone plates and actively assesses implant load under functional weight bearing through the integrated strain sensor for up to eight months. The system additionally consists of a smartphone app for wireless communication with the datalogger via Bluetooth Low-Energy and a cloud server for centralized data collection. The implant system has been used and validated for safety and performance in an animal study²² and are currently applied in a premarket clinical investigation (NCT05410587).

Revision surgery. Anesthesia and aseptic preparation were performed for all the animals at revision in the same manner as for the primary surgery. A skin incision was made on the medial aspect of the tibia, followed by blunt subcutaneous preparation to expose the plate and the osteotomy.

DAIR approach: Visibly infected or necrotic tissue, abscess formations as well as pus were removed with blunt and sharp debridement and sampled for bacterial culture. The implant was cleaned with gauze swabs. All surfaces were then flushed with sterile saline from a bulb syringe (Medline DYND20125). In total, 1 L of sterile saline was used per sheep. The fluid was

collected in single-use suction bags (Medela AG, 077.0083). All the collected samples (debridement tissue and irrigation fluid) were used for bacterial quantification (methods described below).

IML. After flushing the surfaces with sterile saline (1 L), the osteotomy was refreshed using a scalpel blade, and the lavage was repeated. A unicortical hole was drilled in screw hole #4 (not used for plate fixation). Screws #3, 7, and 9 were removed (and sent for bacteriological culture), allowing access to the IML, where the infected issue was retrieved as far as possible using curettes. Tissue plasminogen activator (tPA; Actilyse 20 mg, Boehringer, Switzerland/Activase rt-PA, Roche, Switzerland; 1 mg/ml) was injected into each of the four holes (2 ml per hole) and left for 10 min to degrade fibrin clot in the IMC and support the irrigation of the IMC. After this, the proximal (between holes #3 and #4) and distal (between holes #7 and #9) segments were flushed with sterile saline using a push-and-pull system with two 50 ml syringes. This procedure was repeated between holes #3 and #9 (500 ml of saline in total for the IML). New screws were placed in the screw holes. In total, 1.5 L of saline was used for the IML per sheep. All the collected samples (debridement tissue, irrigation fluid, debridement tissue from IML, irrigation fluid from IML, screws #3, #7, and #9) were used for bacterial quantification as described below.

Blood culture. Ten ml of blood were aseptically sampled from the jugular vein (pre-revision surgery, before IML, post-IML, and 4 h post-IML) and added to the blood culture systems (Oxoid SIGNAL Blood Culture System). Blood culture bottles were cultured at 37 °C while shaking. At 24 h and at 7 days, 200 µl of samples were plated on blood agar (BA) plates (Oxoid). Bacterial growth on BA plates was verified after 24 h of incubation at 37 °C and if culture positive, Staphaurex™ Latex Agglutination Test (ThermoFisher Scientific) test was performed.

Thoracic computed tomography (CT). In the 3 weeks infection groups, clinical CT scans (Revolution EVO, GE Medical Systems (Schweiz) AG, Glattbrugg, Switzerland) of the thorax were performed immediately pre- and post-revision surgery, and 3 days after revision surgery in order to determine whether fat emboli reached the lungs. CT settings were 120 kVp energy, 400 mAs tube current without dose modulation, 0.4 s rotation time, 40 mm detector coverage, a pitch of 0.984:1, and a slice thickness of 0.625 mm. The images were reconstructed with Standard and Lung kernel. Lung CT pre- and post-revision was performed while animals were under anesthesia from the surgery. For the scan 3 days after revision, sheep were anesthetized by IV injection of midazolam (0.15 mg/kg) and propofol (2 mg/kg), afterward intubated, and anesthesia maintained with sevoflurane in oxygen and air. During the scans, animals were placed in dorsal recumbency. During the post-operative scan and the scan 3 days after revision, a CT pulmonary angiography was performed using a bolus tracking technique with the contrast media injector (Ohio tandem, Ulrich medical, Ulm, Germany) and 90 ml of the contrast medium Iomeron 400 mg/ml (Bracco Suisse S.A., Plan-les-Ouates, Switzerland). Briefly, sequential axial slices were obtained at a set region of interest (truncus pulmonalis) during the contrast injection into the jugular vein with a flow rate of 5.5 ml/s until a threshold enhancement (+60 HU) was met, triggering the diagnostic scan.

Analyses of the thoracic CT scans were performed by a boarded veterinary radiologist, who was blinded to sheep pathology and group but not time point. Given that the pulmonary findings were highly subjective, time points were compared when assessing the severity or type of changes. All images were examined in Osirix. Lungs were examined on a standard lung window: WL:−600 WW:1600 slice thickness of 625 µm. Angiography was examined with WL:100 and WW:700, then slice thickness often increased to 2.5 mm, but here, slice thickness was varied. Soft tissues pre-contrast examined with WL:50 and WW:350.

Blood analysis. Blood samples were taken preoperatively and weekly afterwards using EDTA tubes (Sarstedt, Germany). The white blood cell

count was analyzed in the EDTA sample using the vet-abc (Medical solution GmbH, Switzerland).

Post-operative care. Sheep were kept in supportive slings during the whole study to prevent excessive load on the operated leg. A bandage was placed after surgery to protect the wound and was removed after 5–7 days. To alleviate post-operative pain, the animals received 0.05 mg/kg buprenorphine (Bupaq, Streuli Tiergesundheits, Switzerland) intramuscular postoperatively and 6 h later, transdermal Fentanyl (fentanyl patch (Fentanyl-Mepha, Mepha, Switzerland; 2 µg/kg/h) for 72 h and 1.4 mg/kg carprofen (Carprodolor, Virbac, Switzerland) subcutaneously for 5 days. Additional analgesia was administered if deemed necessary due to signs of pain.

During the study, animal welfare was evaluated by the animal caretakers and veterinarians using a scoresheet including the following parameters: behavior, respiration, food uptake/rumination, excretion, bodyweight, weight bearing of the operated leg, and wound healing. After each surgery (index surgery and revision surgery) the animals were closely monitored for any sign of discomfort and scored twice per day until day 5 post op, daily until day 7 post op, then twice weekly until the end of the study. All sheep were weighted weekly or biweekly.

Antibiotics and euthanasia

After revision surgery, the sheep were treated systemically for two weeks with flucloxacillin (2 g/sheep) by iv infusion over 30 min four times a day for 2 weeks (2 g/sheep). Thereafter, sheep were treated for 4 weeks two times a day with rifampicin (600 mg/sheep) as an iv infusion over 1 h followed by slow iv injection of cotrimoxazole 0.6 ml/10 kg bodyweight.

After 2 weeks of antibiotic wash-out, the animals were euthanized by means of iv administration of 20 ml pentobarbital (300 mg/ml, Eskonarcon, Streuli Pharma AG, Switzerland).

Radiography

Radiographs (antero-posterior (AP) and mediolateral (ML) view) were taken post-operatively, before and after revision, and every second week from the beginning of the study. Callus formation of each cortex was evaluated and scored using the modified Radiological Union Scale for Tibia fractures (mRUST) scores²³. AP and ML radiographs of tibia were blindly reviewed by two of the investigators (NV and MM). Assessments were performed on radiographs taken at revision (2, 3, or 5 weeks, depending on the group), six weeks post revision, and at euthanasia. Each cortex is scored as 1 = no callus, 2 = callus present, fracture line visible, 3 = bridging callus, fracture line not visible, 4 = remodeled, fracture not visible. All scores from the individual cortical scores (anterior, posterior, medial, and lateral) are summed up, resulting in a sum score ranging from a minimum score of 4 or a maximum score of 16. Low scores indicate poor fracture healing and callus formation, while high scores correlate with fracture healing and remodeling²⁴.

Tibia CT

CT scans of the operated tibia were performed at different time points for the 5 weeks and 3 weeks infection groups with/without IML. The 5 weeks infection group was scanned post-revision surgery at 5 weeks, afterwards at 8, and at euthanasia. The 3 weeks infection groups were scanned 3 days after revision surgery (together with the lung CT scan), afterwards at 8 weeks, and euthanasia (11 weeks). For the scans at 8 weeks, anesthesia was performed as described for the lung CT. CT settings were 120 kVp energy, 200 mAs tube current without dose modulation, and a slice thickness of 0.625 mm. The images were reconstructed with the bone kernel. A bone mineral density (BMD) calibration phantom (QRM-BDC/6, QRM GmbH, Möhrendorf, Germany) was present in all scans to be able to calibrate the image data from HU to BMD values. Data was analyzed using a current version of Amira (Amira 2021.1, FEI SAS a part of Thermo Fisher Scientific, Hillsboro, Oregon, United States of America) to monitor changes to the osteotomy. The osteotomy gap (Region of Interest, RoI)

was segmented via interpolation between both osteotomy sides for the half-tube opposite the bone plate to minimize metal artifact influence on the evaluation. Subsequent scans were registered to the baseline scans using rigid registration. With the resulting transformation matrix, the RoI was transformed to the respective scans to allow evaluation of the same regions. Bone was segmented automatically (threshold = 400 mgCaHA/ml) and bone volume and BMD were computed within the RoI using direct voxel counting methods. For group 3 weeks + IML, the RoI was redone after revision surgery because, due to the screw removal and replacement, the bone moved slightly relative to the implant and the initial surgery. All image processing and analysis were performed blindly with custom TCL scripts in Amira.

Sample processing for bacteriological analyses and histology

At revision, the debridement tissue and the debridement tissue for the IMC were weighed and then homogenized using 20 ml or 10 ml phosphate buffer saline (PBS), respectively. The irrigation fluids and the screws (in 12 ml of PBS) were sonicated for 10 min using Bandelin Ultrasonic water bath (Model RK 510 H).

At euthanasia, the subcutaneous tissue, bone cores (including one bone core from the osteotomy side and 2 bone cores from the proximal part, and 2 from the distal part), bone marrow, plate, and screws were collected. The bone cores (8 mm diameter) were obtained using a specially designed and custom-made stainless-steel drill (made at the AO Research Institute Davos). The subcutaneous tissue was collected by dissecting all tissue above the plate, while the complete bone marrow was collected using a curette after separating the proximal and distal bone parts at the osteotomy. All the tissue samples, aside from the plate and screws, were weighed, and afterward, 20 ml of PBS was added to all the tissues. Subcutaneous tissue and bone marrow samples were first homogenized and then sonicated for 10 min as described above. For the plate and screw sample, 60 ml of PBS was added and then sonicated. When present, 20 ml of PBS was added to the sensor but never sonicated. Bacteria were diluted to spot inoculate 10 µl of each dilution on BA plates and incubated overnight at 37 °C to quantify the surviving population ($n = 3$ per sample). Undiluted samples (200 µl) were also plated on a BA plate. In case of a negative result in the undiluted BA plate, the samples were filtered through a membrane, and the membrane was cultured on the BA plate overnight, allowing the total number of bacteria/samples to be enumerated.

Identification of *S. aureus* in culture-positive samples was performed for at least one colony from each culture-positive animal, using Staphaurex™ Latex Agglutination Test (Thermo Fisher).

Additional bone cores were collected from the osteotomy site for histological analyses. One sample was fixed and processed for Giemsa & Eosin (G&E) staining, while a second one was fixed, decalcified, and processed for Brenn and Brown (BB) staining and tartrate-resistant acid phosphatase (TRAP) staining, which allows the visualization of osteoclasts.

In vitro assays

Cell viability of human fibroblasts with tPA. Telomerase-immortalized human foreskin fibroblasts (hTERT-BJ1) were used to test the biocompatibility of tPA. hTERT-BJ1 were purchased from Clontech (USA) and were routinely cultured as previously described²⁵. Briefly, hTERT-BJ1 was cultivated in alpha-Minimum Essential Medium (α-MEM) (Gibco, USA) supplemented with 10% fetal bovine serum (Corning) with the addition of 100 µg/mL streptomycin (Gibco), 100 U/mL penicillin (Gibco) at 37 °C in a humidified 5% CO₂ atmosphere. Three different concentrations of tPA were tested: 0.01, 0.1, 1, and 10 mg/ml. tPA was dissolved in α-MEM and applied to the cells. As positive controls, cells were grown in a complete medium (α-MEM, 10% FBS, and 1% P/S) without any tPA. Cells treated with dimethyl sulfoxide (Sigma-Aldrich, USA) were used as negative controls. To determine cell viability, CellTiter-Blue (Promega, USA) was used on days 1, 3, and 7 following the manufacturer's instructions. Cell viability (calculated in %) was determined as the fluorescence ratio between

cells exposed to different concentrations of tPA and the positive control. The experiment was performed in triplicate.

Biofilm assay with tPA

Biofilm of *S. aureus* ATCC 25923 was grown on metal discs for 48 h and then exposed to tPA and/or flucloxacillin. Briefly, *S. aureus* ATCC 25923 was grown overnight in TSB at 37 °C with agitation at 100 rpm. The following day, the bacterial culture was centrifuged at 3220 rcf for 7 min, washed once with PBS, and then finally resuspended in TSB. After 3 min sonication, the OD₆₀₀ was adjusted to 0.01, and 1 ml of this culture was added to each metal disc. The biofilm was allowed to grow at 37 °C for 48 h and then the different conditions were applied: 15 min tPA treatment (1 mg/ml) with or without flucloxacillin (100× minimum inhibitory concentrations (MIC), MIC 0.5 µg/ml) treatment (24 h) or tobramycin (100× MIC–MIC: 1 µg/ml) compared only antibiotic treatment or controls. At 72 h, the metal discs were sonicated in PBS and solutions were diluted to spot inoculate 10 µL of each dilution on tryptic soy agar plates to quantify the surviving population.

Statistics

GraphPad Prism 9 was used for all statistical analyses. For all tests, each group from each dataset was tested for normal distribution with the following tests: Anderson-Darling test, D'Agostino and Pearson test, Shapiro–Wilk test, and Kolmogorov–Smirnov test. If one group from a dataset did not pass the normal distribution on one of these four tests, then the dataset was considered as not normally distributed. According to these criteria, all datasets were not normally distributed, so a non-parametric Mann–Whitney test, Dunn's multiple comparison test, or two-way analysis of variance with Šidák's multiple comparisons test were used to determine statistical differences between the groups of each dataset. Only significant statistical differences are displayed in the figures.

Study approval

The study was approved by relevant Swiss authorities (Cantonal authorities of Grisons, Switzerland: Permission # 07_2020, 22_2021) and performed in a facility accredited by the Association for Assessment and Accreditation of Laboratory Animal Care International (AAALAC). ARRIVE guidelines checklist is included in the supplement material.

Data availability

All data generated or analyzed during this study are included in this published article [and its supplementary information files]. The raw data generated and/or analyzed during the current study are available in the supplementary file.

Received: 12 August 2024; Accepted: 29 December 2024;

Published online: 24 February 2025

References

1. Depypere, M. et al. Pathogenesis and management of fracture-related infection. *Clin. Microbiol. Infect.* **26**, 572–578 (2020).
2. Trampuz, A. & Zimmerli, W. Diagnosis and treatment of infections associated with fracture-fixation devices. *Injury* **37**, S59–S66 (2006). Suppl 2.
3. Yokoyama, K., Itoman, M., Shindo, M. & Kai, H. Contributing factors influencing type III open tibial fractures. *J. Trauma* **38**, 788–793 (1995).
4. Metsemakers, W. J. et al. Fracture-related infection: A consensus on definition from an international expert group. *Injury* **49**, 505–510 (2018).
5. Metsemakers, W. J. et al. g. Fracture-Related Infection, General treatment principles for fracture-related infection: recommendations from an international expert group. *Arch. Orthop. Trauma. Surg.* **140**, 1013–1027 (2020).
6. Buijs, M. A. S. et al. Outcome and risk factors for recurrence of early onset fracture-related infections treated with debridement, antibiotics

- and implant retention: Results of a large retrospective multicentre cohort study. *Injury* **53**, 3930–3937 (2022).
7. Berkes, M. et al. Fracture, Maintenance of hardware after early postoperative infection following fracture internal fixation. *J. Bone Joint. Surg. Am.* **92**, 823–828 (2010).
 8. Willenegger, H. & Roth, B. Treatment tactics and late results in early infection following osteosynthesis. *Unfallchirurgie* **12**, 241–246 (1986).
 9. Morgenstern, M. et al. The influence of duration of infection on outcome of debridement and implant retention in fracture-related infection. *Bone Joint J* **103-B**, 213–221 (2021).
 10. Metsemakers, W. J. et al. Infection after fracture fixation: Current surgical and microbiological concepts. *Injury* **49**, 511–522 (2018).
 11. Cox, G., Jones, E., McGonagle, D. & Giannoudis, P. V. Reamer-irrigator-aspirator indications and clinical results: a systematic review. *Int. Orthop.* **35**, 951–956 (2011).
 12. Lempert, M. et al. Incidence of Fat Embolism Syndrome in Femur Fractures and Its Associated Risk Factors over Time-A Systematic Review, *J Clin. Med.* **10**, (2021).
 13. Akoh, C. C., Schick, C., Otero, J. & Karam, M. Fat embolism syndrome after femur fracture fixation: a case report. *Iowa. Orthop. J.* **34**, 55–62 (2014).
 14. Kuehl, R. et al. Time-dependent differences in management and microbiology of orthopaedic internal fixation-associated infections: an observational prospective study with 229 patients. *Clin. Microbiol. Infect.* **25**, 76–81 (2019).
 15. de Mesy Bentley, K. L., MacDonald, A., Schwarz, E. M. & Oh, I. Chronic Osteomyelitis with Staphylococcus aureus Deformation in Submicron Canaliculi of Osteocytes: A Case Report. *JBJS Case Connect* **8**, e8 (2018).
 16. de Mesy Bentley, K. L. et al. Evidence of Staphylococcus Aureus Deformation, Proliferation, and Migration in Canaliculi of Live Cortical Bone in Murine Models of Osteomyelitis. *J. Bone Miner. Res.* **32**, 985–990 (2017).
 17. Jensen, L. K., Birch, J. M., Jensen, H. E., Kirketerp-Moller, K. & Gottlieb, H. Bacterial invasion of the submicron osteocyte lacuna-canalicular network (OLCN): a part of osteomyelitis disease biology. *APMIS* **131**, 325–332 (2023).
 18. Puetzler, J. et al. Implant retention in a rabbit model of fracture-related infection. *Bone Joint. Res.* **13**, 127–135 (2024).
 19. Ernst, M., Richards, R. G. & Windolf, M. Smart implants in fracture care - only buzzword or real opportunity? *Injury* **52**, S101–S105 (2021). Suppl 2.
 20. Kienast, B. et al. An electronically instrumented internal fixator for the assessment of bone healing. *Bone. Joint. Res.* **5**, 191–197 (2016).
 21. Ernst, M. et al. Clinical feasibility of fracture healing assessment through continuous monitoring of implant load. *J. Biomech.* **116**, 110188 (2021).
 22. Windolf, M. et al. Continuous Implant Load Monitoring to Assess Bone Healing Status-Evidence from Animal Testing. *Medicina (Kaunas)* **58**, 858 (2022).
 23. Litrenta, J. et al. Determination of Radiographic Healing: An Assessment of Consistency Using RUST and Modified RUST in Metadiaphyseal Fractures. *J. Orthop. Trauma.* **29**, 516–520 (2015).
 24. Plumarom, Y. et al. Sensitivity and specificity of modified RUST score using clinical and radiographic findings as a gold standard. *Bone Joint Open* **2**, 796–805 (2021).

25. Meredith, D. O. et al. Human fibroblast reactions to standard and electropolished titanium and Ti-6Al-7Nb, and electropolished stainless steel. *J. Biomed. Mater. Res. A* **75**, 541–555 (2005).

Acknowledgements

The authors would like to thank Pamela Furlong and Iris Keller for their technical support for microscopy and the bacteriological analyses, Nora Goudsouzian and Mauro Bluvo for histology, and Dirk Nehrbass for histopathology. Special thanks to all the surgical team veterinarians and animal caretakers at the preclinical services of the AO Research Institute Davos.

Author contributions

C.S.: designing research studies, conducting experiments, acquiring data, analyzing data, providing reagents, and writing the manuscript; L.G. and T.B.: conducting and planning animal studies; C.C.: conducting animal studies; M.E.: acquiring and analyzing sensor data; D.G.: acquiring and analyzing CT data; M.M.: analyzing and scoring radiographs and revision of the manuscript; G.R.: review manuscript; H.R.: lung. C.T. data analyses; N.V.: analyzing and scoring radiographs; M.W.: lung CT data analyses; M.W.: sensor development; S.Z.: conducting and planning animal studies; F.M.: designing research studies, revision of the manuscript. All authors have read and approved the manuscript.

Competing interests

The authors declare no competing interests.

Additional information

Supplementary information The online version contains supplementary material available at <https://doi.org/10.1038/s41522-024-00643-0>.

Correspondence and requests for materials should be addressed to T. Fintan Moriarty.

Reprints and permissions information is available at <http://www.nature.com/reprints>

Publisher's note Springer Nature remains neutral with regard to jurisdictional claims in published maps and institutional affiliations.

Open Access This article is licensed under a Creative Commons Attribution-NonCommercial-NoDerivatives 4.0 International License, which permits any non-commercial use, sharing, distribution and reproduction in any medium or format, as long as you give appropriate credit to the original author(s) and the source, provide a link to the Creative Commons licence, and indicate if you modified the licensed material. You do not have permission under this licence to share adapted material derived from this article or parts of it. The images or other third party material in this article are included in the article's Creative Commons licence, unless indicated otherwise in a credit line to the material. If material is not included in the article's Creative Commons licence and your intended use is not permitted by statutory regulation or exceeds the permitted use, you will need to obtain permission directly from the copyright holder. To view a copy of this licence, visit <http://creativecommons.org/licenses/by-nc-nd/4.0/>.

© The Author(s) 2025